Published in final edited form as:
Neuron. 2011 December 22; 72(6): 991–1000. doi:10.1016/j.neuron.2011.11.014.

The pore of the voltage-gated proton channel

Thomas K. Berger[1] and **Ehud Y. Isacoff**[1,2,*]

[1]Department of Molecular and Cell Biology and Helen Wills Neuroscience Institute, 142 Life Sciences Addition, University of California, Berkeley, CA 94720

[2]Physical Bioscience Division, Lawrence Berkeley National Laboratory, Berkeley, CA 94720

SUMMARY

In classical tetrameric voltage-gated ion channels four voltage-sensing domains (VSDs), one from each subunit, control one ion permeation pathway formed by four pore domains. The Hv proton channel has a different architecture, containing a VSD, but lacking a pore domain. Since its location is not known, we searched for the Hv permeation pathway. We find that mutation of the S4 segment's third arginine R211 (R3) compromises proton selectivity, enabling conduction of a metal cation and even of the large organic cation guanidinium, reminiscent of Shaker's omega pore. In the open state, R3 appears to interact with an aspartate (D112) that is situated in the middle of S1 and is unique to Hv channels. The double mutation of both residues further compromises cation selectivity. We propose that membrane depolarization reversibly positions R3 next to D112 in the transmembrane VSD to form the ion selectivity filter in the channel's open conformation.

INTRODUCTION

Voltage-gated proton channels are broadly expressed in many tissues and across phyla [DeCoursey, 2008]. They participate in acid extrusion from neurons, muscles, and epithelial cells [DeCoursey, 2003], as well as in reactive oxygen species production by the NADPH oxidase in phagocytes [Henderson et al., 1987, DeCoursey et al., 2003, Ramsey et al., 2009]. The first member of the voltage-gated proton channel family to be cloned, Hv1 [Ramsey et al., 2006, Sasaki et al., 2006], contains the typical four transmembrane segments (S1, S2, S3 and S4) of a voltage-sensing domain (VSD), but lacks the two transmembrane segments (S5 and S6) and the intervening re-entrant pore (P) loop that together form the pore domain in other voltage-gated channels (Figure 1). Nevertheless, the purified Hv1 protein can be functionally reconstituted in artificial lipid bilayers, indicating that it contains all of the functional domains of the channel [Lee et al., 2009]. Hv1 assembles as a homo-dimer [Tombola et al., 2008, Koch et al., 2008, Lee et al., 2008] due to a coiled-coil dimerization domain in its cytoplasmic C-terminal domain [Li et al., 2010]. Disruption or replacement of the coiled-coil domain renders the channel monomeric, but retains functionality, indicating that a pore must be contained within an individual VSD [Tombola et al., 2008, Koch et al., 2008] (Figure 1A). Indeed, in the dimeric channel, whose two pores gate cooperatively [Tombola et al., 2010, Gonzalez et al., 2010], the pores can be blocked individually by site-specific attachment of cysteine-reactive probes [Tombola et al., 2008]. Thus, it is clear that

*To whom correspondence should be addressed: ehud@berkeley.edu .

the VSD of Hv1—the only transmembrane portion of the protein—must contain the pore. However, the precise location of the proton permeation pathway has yet to be elucidated.

We searched for the permeation pathway in the human Hv1 channel by looking for the portion of the VSD that confers ion selectivity. Proton channels are extremely selective, able to generate large proton currents while excluding Na^+ and K^+, despite the fact that Na^+ and K^+ are present in greater than one million-fold higher concentrations than are protons at physiological pH.

We find that mutations that alter R211, the S4 segment's third arginine (R3), enable the channel to conduct the large organic cation guanidinium. We also obtain evidence suggesting that an aspartate that is unique to Hv channels (D112), which is situated in the middle of S1, interacts with R3. Interestingly, mutation of D112 also alters ion selectivity. These findings suggest that R3 and D112 contribute to the narrowest part of the transmembrane pathway to form the ion selectivity filter of the channel. Given that the S4 of Hv1 moves outward in response to depolarization [Gonzalez et al., 2010], as is the case with the classical tetrameric voltage-gated channels [Tombola et al., 2006], we propose that opening of the channel involves the formation of the selectivity filter when S4 motion places R3 into interaction with D112 in the narrowest part of the pore.

RESULTS

We set out to search for the location of the Hv1 pore. We focused our initial attention on arginines in S4 because earlier work on the VSD of the Shaker K^+ channel showed that substitution with histidine creates a proton selective conductance [Starace and Bezanilla, 2001, Starace and Bezanilla, 2004] and substitution with uncharged, smaller side chains creates a non-selective cation conductance [Tombola et al., 2005], with one such pore in each VSD [Tombola et al., 2007]. A similar cation conductance is found in naturally occurring disease mutants of S4 arginines in Na^+ channel [Sokolov et al., 2005, Struyk et al., 2008].

The S4 of Hv1 contains three arginines: R205 (R1), R208 (R2) and R211 (R3) (Figure 1A,B). Three residues after R3 Hv1 has an asparagine, N214 (N4), which, depending on the sequence alignment, is either in register with lysine "K5" (Figure 1B) or R4 of the classical tetrameric voltage-gated channels. Both R3 and N4 are predicted by earlier work [Gonzalez et al., 2010] to lie within the span of the membrane at positive voltage, so that, in principle, either or both could lie in the pore in the open state. By analogy with the conductance properties of the Shaker K^+ channel VSD, however, the arginine at R3 would be incompatible with the conductance of cations, including protons, but the neutral asparagine at N4 may be compatible. We examined both positions.

The R3S mutant permeates a large cation

We began by following up on the earlier finding that the large organic cation, guanidinium (Gu^+), blocks proton efflux through the Hv1 channel [Tombola et al., 2008], suggesting that Gu^+ might enter the internal mouth of the pore from the internal solution, but might be too large to pass through it. We reasoned that mutations that widened the pore might let Gu^+ permeate and would thereby identify the residues that line the pore.

In symmetric pH 8.0 solutions, with 100 mM Gu^+ in the internal solution only, the wildtype (WT) channel did not conduct outward current (Figure 2A and Figure S1). Mutation of N4 to serine (N4S) did not alter this behavior (Figure 2A). In contrast, mutation of R3 to serine (R3S) led to large voltage dependent outward currents (Figure 2A,B), suggesting that this mutation enables Gu^+ to permeate the pore. To test whether Gu^+ was actually the

permeating cation (and not protons), we measured tail currents evoked by a large depolarizing step, at different tail potentials (Figure 2C). In symmetric pH 8, the reversal potential of the tail currents of R3S depended on the balance between internal and external Gu^+ concentrations, closely approximating the predicted equilibrium potential for Gu^+ (Figure 2C,D). This indicates that Gu^+ is the main conducting ion in R3S in symmetric pH 8.

We tested the role of R3 in selectivity with mutation to 15 other amino acid identities, including non-polar, polar and positively charged side chains. We found that all of the mutants (glycine, alanine, cysteine, leucine, methionine, tryptophan, proline, serine, threonine, asparagine, glutamine, tyrosine, aspartate, histidine and lysine) support voltage-dependent current in 100 mM Gu^+ (Figure S1). Thus, the native arginine at R3 is uniquely suited to prevent Gu^+ conduction at pH 8.

R3S mutation specific to selectivity

Two defining features of intact proton channels are a high sensitivity to external Zn^{2+} [Ramsey et al., 2006, Sasaki et al., 2006] as well as gating that depends on the pH gradient across the membrane [Ramsey et al., 2010]. We found that both of these features were preserved in the R3S mutant channel. First, we found that proton current through the R3S mutant measured at symmetric pH 6 was efficiently inhibited by external Zn^{2+}. Application of 100 μM external Zn^{2+} reduced the proton current by 99.9 ± 0.01 % (n = 3) (Figure 3A). This degree of inhibition is similar to what has been observed in the WT channel [Ramsey et al., 2006]. Second, outside-out recordings that started in symmetric pH 6, where external pH was increased successively to 7 and then 8, showed that the voltage dependence of gating of the R3S mutant is shifted by −48.9 ± 1.2 mV per pH unit (Figure 3C). This value is similar to what has been determined for the WT channel [Ramsey et al., 2010], showing that the R3S mutant maintains the normal sensing of the transmembrane pH gradient. Thus, two of the characteristic features of Hv1 are preserved in the R3S mutant channel, consistent with a specific effect of the mutation on selectivity.

Protons and Gu^+ permeate through the same pathway in mutants of R3

Having seen that the R3S mutant conducts Gu^+ ions, we next asked whether the conduction pathway for these ions is the same as the native pathway for protons. In other words, does the R3S mutation compromise the selectivity of the proton conduction pathway, or does it create a separate pathway for conduction of Gu^+? We first asked whether external Zn^{2+} inhibited the Gu^+ current through the R3S mutant channel since it inhibits the proton current. At $pH_i = pH_o = 8$ and symmetric 100 mM Gu^+, where Gu^+ is the main charge carrier (Figure 2C,D), we found that 100 μM external Zn^{2+} inhibited the current by 98.4 ± 0.7 % (n = 3) (Figure 3B), similar to the degree of inhibition of the proton current through R3S (Figure 3A). This supports the notion that the R3S mutation permits Gu^+ to permeate through the proton pathway.

To further test the interpretation that protons and Gu^+ permeate through the same pathway in R3S, we examined interactions between proton and Gu^+ conduction in this mutant. As shown previously [Tombola et al., 2008], internal 10 mM Gu^+ blocks outward proton conduction in WT hHv1 (by 32.5 ± 3.3 % at $pH_i = pH_o = 6$, n = 6) (Figure 4A). We found that a similar block of outward proton current by internal 10 mM Gu^+ occurs in R3S (25.6 ± 4.7 % for $pH_i = pH_o = 6$, n = 4) (Figure 4A), showing no significant difference from the proton block of WT (p = 0.25, t-test). This suggests that protons and Gu^+ take the same pathway, but that the relatively low Gu^+ conduction rate in the R3S mutant obstructs the flow of protons when both are present and protons are the main charge carrier.

The results so far suggest that alteration of the R3 side chain permits permeation by Gu^+ through the proton pathway. To test this idea explicitly, we designed an experiment that would permit a blocker to be molecularly targeted to the R3 location of S4. We did this by substituting a cysteine instead of a serine at the R3 position, enabling the residue to be derivatized. We found that, like R3S, R3C retained the characteristic properties inhibition by external Zn^{2+} and the sensitivity of gating to the pH gradient (Figure S2). Moreover, like R3S, R3C also conducts Gu^+ (Figure S3). Following baseline recording of current through R3C channels in inside-out patches, we exposed the inner face of the membrane to the positively charged, thiol-reactive (2-(Trimethylammonium)ethyl) methanethiosulfonate (MTSET). Internal MTSET blocked conduction of both protons and Gu^+ conduction in R3C channels, though to somewhat different degrees (by 93.1 ± 3.0 %, n = 6 and 66.0 ± 3.7 %, n = 7, respectively) (Figure 4B). The observations support the notion that protons and Gu^+ have a single common pathway and that, in the open state of the channel, R3 creates a barrier in a narrow stretch of the pore to Gu^+, while permitting passage of protons. The MTSET adduct attached to cysteine at this position functions as a barrier to both protons and Gu^+, but one that is less effective than the shorter and bulkier native arginine side chain against Gu^+.

“Double-gap” not needed for conduction

To permit an omega current through the Shaker K^+ channel VSDs requires a “double gap” (absence of arginine in two consecutive positions within S4’s repeating sequence of an arginine at every third position) [Gamal El-Din et al., 2010]. If this were also the case in Hv1, then substitution of N4 with arginine in the R3S background should prevent conduction of Gu^+ by bracketing the R3 position with arginines: the native R2 immediately before and an introduced R4 immediately after R3. However, we found that, in the R3S background, the N4R mutation (i.e. the double mutation R3S-N4R) not only preserved proton conduction but did not prevent conduction by Gu^+ (Figure S4). This finding suggests that the narrow part of the Hv1 conducting pathway is particularly short.

R3 interacts with D112

If R3 were positioned in the narrow part of the pore in the activated state, as its homologs are in the VSDs of Shaker [Larsson et al., 1996, Baker et al., 1998, Gamal El-Din et al., 2010] and Kv1.2 [Long et al., 2007] K^+ channels and Na^+ channels [Yang et al., 1996, Sokolov et al., 2005], it would be predicted to have a counter-charged partner from one of the other transmembrane segments. The partner residue for R3 in Kv1 channels—a conserved glutamate in the outer third of S2 (E283 in Shaker, E226 in Kv1.2) [Tiwari-Woodruff et al., 2000, Long et al., 2007]—is also present in Na^+ channels [DeCaen et al., 2008], but is missing in Hv1. Instead, Hv1 has a unique aspartate, D112, located in the middle of S1, which is conserved in proton channels (Figure 1B), and has been predicted by homology modeling to face R3 in the activated state [Ramsey et al., 2010]. Mutation of D112 to alanine was earlier shown to shift the conductance-voltage relation (G-V) strongly in the positive direction [Ramsey et al., 2010]. We found that mutation of D112 to serine had such a strong effect that a step to +150 mV evoked outward current of <50 pA at pH_i = pH_o = 6 (Figure 5A). We also found that the G-V of R3S is substantially shifted in the depolarized direction (Figure 5A). Strikingly, combining the two mutations in the double mutant D112S-R3S shifted the G-V in the negative direction to be close to that of WT channels (Figure 5A,B). D112S-R3S was found to retain the pH gradient sensing and external Zn^{2+} sensitivity of the WT channel (Figure S2), and also to conduct Gu^+ like R3S and R3C (Figure S3). These results suggest that D112 interacts with R3 in the open state of the channel and that loss of charge at one of the pair destabilizes the open state, whereas loss of both restores open state stability.

If D112 interacted with R3, as deduced above, then one would predict that a substitution of the aspartate at D112 with glutamate would retain a relatively normal G-V because it retained the negative charge. This was indeed observed in the single mutant D112E (Figure 5A).

If our inferences so far are correct, and R3 and D112 interact in the open conformation, with R3 lining the pore, then D112 would also be expected to line the open pore. We tested this expectation by considering our observation that substitution of R3 with any of a variety of different amino acids leads to outward current in the high Gu^+ solution, i.e. loss of ion selectivity (Figure S1). This led us to predict that a mutation at R3 that has lost ion selectivity should have the selectivity restored if a complementary mutation could be made at D112 that would re-establish an interaction. If the interaction between D112 and R3 were electrostatic, then a charge reversal would provide a good test. Since, as seen with the 14 other substitutions made initially at R3, a mutation of R3 to aspartate (R3D) also compromises ion selectivity, giving rise to outward current at 100 mM Gu^+ at pH 8 (Figures S1 and 6), we tested the effect of a charge reversal. Strikingly, the addition of the mutation D112R to the selectivity-compromised R3D to generate the double mutant D112R-R3D (thus swapping the charges between D112 and R3) yielded a channel with an outward current at $pH_i = 6$, $pH_o = 8$, but not with 100 mM Gu^+ pH 8 as the internal solution (Figure 6). In other words, the introduction of the charge reversal by the D112R mutation complemented the effect of the R3D charge reversal and restored proton selectivity (Gu^+ exclusion), as predicted for an interaction between D112 and R3 in the open state of the channel.

Influence of D112 and R3 on selectivity

Based on what we have seen so far, the contribution of D112 to ion selectivity could be explained by an indirect effect of D112 on the role of R3 in selectivity. We next set out to determine if D112 has a direct effect on selectivity. To do this we extended our analysis to metal cations and compared the conductance of WT channels and channels mutated at either R3 alone or both R3 and D112. Our first approach was to test outward currents elicited by voltage steps (to +60 mV) in patches where the pipette was filled (external solution) with 100 mM NaCl solution and to sequentially test 100 mM internal Na^+, Li^+, K^+, Cs^+ and Gu^+. The experiment was carried out in symmetric pH 8 to minimize contribution by proton current.

WT channels supported outward current in the presence of the metal cations, with modestly larger currents in Na^+, K^+, and Cs^+ than in Li^+ (Figure 7A). In Gu^+, current was almost entirely abolished (reduction to 8.6 ± 1.4 %, n = 8) (Figure 7A), consistent with pore block, as shown above (Figure 2A and S1). To assess the fraction of the metal ion current that was carried by protons we switched the internal solution of patches between 100 mM TRIS pH 8 (protons alone) and 100 mM Na^+ pH 8 (i.e. Na^+ plus protons). We observed little change in Na^+ current (Figure S5), suggesting that most of the current of WT channels in the presence of metal ions is carried by protons (Figure 7A, dashed line).

In contrast to WT, R3S channels had currents in Gu^+ that were almost 9-fold larger than in Li^+ (Figure 7B). Moreover, unlike WT, in the presence of metal ions, R3S current was largest in Li^+ (Figure 7B) (*e.g.* the K^+/Li^+ ratio was 1.32 ± 0.07 for WT *versus* 0.24 ± 0.02 for R3S, n = 8 and n =11, respectively, $p < 0.01$). The 100 mM TRIS pH 8 (protons alone) *versus* 100 mM Na^+ pH 8 (i.e. Na^+ plus protons) ratio was also close to unity in R3S (Figure S5), suggesting that the R3S mutation increases permeability to Li^+ (Figure 7B, bottom, dashed line).

To examine D112 we first turned to the D112S mutant, but its current was too small (Figure 5). Since the charge conserving D112E mutation did not shift the G-V (Figure 5), the substituted glutamate of this mutant seems to accommodate the normal interactions of the native aspartate. If the model was correct and pairing between R3 and D112 were important for selectivity, one would expect the D112E mutant to retain normal selectivity. This was indeed the case. The D112E mutant had no appreciable conductance in Gu^+ and the order of current amplitudes in the different metal cations closely resembled that of WT (Figure 7D). We therefore turned to the D112S-R3S double mutant. In D112S-R3S, the current of Gu^+ was more than 14-fold larger than that of Li^+ (Figure 7C). This value is significantly larger than what is seen in R3S alone (Gu^+ / Li^+ ratio: R3S, 8.69 ± 0.45, n = 11; D112S-R3S, 14.25 ± 1.77, n = 8; $p < 0.01$, t-test). Strikingly, assessment of the protons alone *versus* Na^+ plus protons ratio indicated that, unlike WT and R3S channels, most of the D112S-R3S current in presence of Na^+ is actually carried by Na^+ (Figure S5, the proton / [proton + 100 mM Na^+] ratio was 0.22 ± 0.03, n = 5 for D112S-R3S, significantly different from both 0.82 ± 0.06, n = 7 for R3S and 0.80 ± 0.05 for WT, $p < 0.01$, ANOVA followed by Dunn's method for multiple comparison).

To test more precisely the effects on ion selectivity of R3 and D112, we examined the reversal potentials of tail currents under mono- and bi-ionic conditions. In WT channels there was no Gu^+ conduction and reversal potentials did not differ between Na^+ and Li^+ (E_{rev} shift = 0.57 ± 1.20 mV, n = 4, p = 0.67, paired t-test), consistent with the analysis above, that indicated that in Na^+ and Li^+ the current is mainly carried by protons. In R3S the reversal potential shift between Na^+ and Li^+ was larger and statistically significant (E_{rev} shift = −4.24 ± 1.70 mV, n = 8, p = 0.04, paired t-test). In D112S-R3S the reversal potential shift between Na^+ and Li^+ increased even more (E_{rev} shift = −13.91 ± 2.30 mV, n = 5, $p < 0.01$, paired t-test) (Figure 8A), indicating significant permeation of Li^+ ions. As expected from the results above (Figure 7), the reversal potential shift between Na^+ and Gu^+ was highly significant for both R3S (E_{rev} shift = −42.11 ± 3.39 mV, n = 5, $p < 0.01$, paired t-test) and D112S-R3S (E_{rev} shift = −58.16 ± 4.28 mV, n = 4, $p < 0.01$, paired t-test). Both, the Li^+ shift and the Gu^+ shift differed significantly between R3S and D112S-R3S (Li^+, $p < 0.01$; Gu^+, p = 0.02, t-tests), indicating that D112S (in combination with R3S) compromises selectivity against both Gu^+ and Li^+. These results indicate that both R3 and D112 influence the cation selectivity of hHv1, consistent with their localization in the narrow part of the pore.

DISCUSSION

The Hv1 proton channel has a VSD as its only membrane spanning region. This indicates that its pore and gate must be located along with its voltage sensor in the VSD, but the location of the pore was unknown. We searched for the Hv1 pore by seeking the portion of the VSD that confers ion selectivity. We began with a focus on S4 arginine positions because earlier work on the VSDs of K^+ and Na^+ channels showed that amino acid substitutions of one or more arginines creates an ion conducting pathway (also known as a "gating pore" or "omega pore") through the VSD [Starace and Bezanilla, 2001, Starace and Bezanilla, 2004, Tombola et al., 2005, Sokolov et al., 2005, Sokolov et al., 2007, Tombola et al., 2007, Struyk et al., 2008, Gamal El-Din et al., 2010]. This suggested to us that a similar pathway could exist in the open state of the WT Hv1 channel to allow for proton permeation.

A charge pair as the selectivity filter

State-dependent cysteine accessibility analysis in Hv1 has shown that S4 moves outward upon membrane depolarization [Gonzalez et al., 2010], as shown earlier for Na^+ and K^+ channels [Tombola et al., 2006]. We examined arginine positions expected to reside within

the span of the membrane in the open state and found that one of these, R211, the third arginine in S4 (R3), plays a role in preventing conductance by both metal cations and the large organic cation guanidinium. We found that an aspartate that resides in the middle of S1, and which is unique to Hv channels (D112), interacts with R3. This interaction is likely to be electrostatic, since mutation D112E preserves both the voltage-conductance relationship as well as proton selectivity. We also find that D112 contributes to ion selectivity, helping to exclude metal cations and guanidinium. The role we find for D112 in selectivity against cations other than protons is interesting given the recent finding that D112 appears to play a role in preventing conduction by anions [Musset et al., 2011].

Mutation of either R3 or D112 alone destabilizes the open state of the channel. When the two residues are mutated at the same time to the small polar residue serine, or when their identities are swapped, so that R3 becomes an aspartate and D112 an arginine, the open state is re-stabilized. These results suggest that R3 and D112 interact in the open state of the channel. While the double mutation of R3 and D112 to serine (D112S-R3S) produced the largest disruption that we observed of ion selectivity, the charge swap (D112R-R3D) retained proton selectivity. Together, these observations suggest that D112 and R3 interact electrostatically to contribute to the selectivity filter of the channel, and that mutation of R3 alone or in combination with D112S induces a voltage sensor that leaks cations other than protons (Figure 8B).

Omega pore occluded by a single arginine

The number of mutations required to create a pore in a VSD provides information on the length and shape of the pore's most constricted site. The "omega pore" through the VSD of the Shaker K^+ channel requires a single mutation of the first arginine R1 to a small side chain [Tombola et al., 2005], leading to its opening when S4 is in the "down state" at hyperpolarized potentials. However, it appears that Shaker actually requires a double gap (substitution of two arginines) and that the outermost position (three residues before Shaker's R1) is naturally "missing" (i.e. is an alanine), while an omega pore can also be made in Shaker at other voltages by mutations at neighboring pairs or arginines [Gamal El-Din et al., 2010]. A double gap is also needed to create an omega pore through the VSD in domain II of $Na_v1.2a$, [Sokolov et al., 2005]. However, in domain II of $Na_v1.4$ channels, mutation of a single arginine (R2 or R3) is sufficient to make an omega current [Struyk et al., 2008, Sokolov et al., 2008, Sokolov et al., 2010]. We find that a single gap is sufficient for hHv1 to conduct Gu^+, indicating that the pore of hHv1 is relatively short.

As we observe here with hHv1, the Shaker omega pore is more permeable to Gu^+ than to metal cations [Tombola et al., 2005]. Moreover, Gu^+ and protons have been found to be highly permeable through the VSD of domain II of $Na_v1.4$ Na^+ channel when a single arginine gap is made by substitution with glycine or histidine [Sokolov et al., 2010]. Thus, the hHv1 VSD pore pathway shares with its counterparts from K^+ and Na^+ channels a preference for the free ion that resembles the arginine side chain. A remarkable feature that appears to distinguish the omega pore of hHv1 from that of other channels is that arginine is uniquely able to select against Gu^+, whereas other bulky or charged residues do not.

Recent molecular dynamics simulations based on homology models built upon voltage-gated K^+ channel crystal structures showed that water can occupy the core of the VSD of hHv1, but not of VSDs of tetrameric channels, suggesting that hHv1 may have evolved a specialized watery proton transfer pathway [Ramsey et al., 2010]. Our findings are compatible with such a transfer pathway and with details of the homology model on which the simulations were based on, namely the close proximity of D112 to R3 in the activated state. Our results suggest that R3 sits at the most constricted site of the water canal, allowing only protons to pass, so that its mutation induces a widening of the water canal, allowing

Gu^+ conduction. In this context the effect of MTSET on R3C is of interest. Whereas MTSET at R3C blocks proton current by more than 90 % (at pH 6), Gu^+ current (at pH 8) is only blocked by about two-thirds. Combined with our observation that the hHv1 selectivity mutants are more permeable to Gu^+ than to smaller metal cations and that arginine at R3 is unique in preventing Gu^+ conduction, this suggests that selectivity depends on more than size exclusion. Another factor in proton selection could involve charge transfer via titration of one or more amino acid side chains, as shown to form a proton-selective omega pore in the Shaker VSD when single arginines are substituted with histidine [Starace and Bezanilla, 2001, Starace and Bezanilla, 2004]. Indeed, D112 was recently proposed to be such a titratable residue, although some proton permeation was preserved when D112 was mutated to non-titratable residues [Musset et al., 2011]. In this case the change from the native arginine at R3 to the longer combined side chain of R3C with the appended MTSET would need to explain a change in the titration of D112 that virtually abolishes proton conduction. Additional work will be required to determine the contribution to selectivity of a constricted watery canal *versus* side chain titration, or, alternatively, a possible contribution of MTSET on gating.

Two alignments of S4 between hHv1 and the $K_V1.2$ K^+ channel have been suggested, creating some uncertainty about the environment and interaction partners of the arginines and their role in proton conduction [Wood et al., 2011]. In suggesting an electrostatic interaction between R3 and D112 in the open state of the channel, our results argue for an alignment that maps the R3 of hHv1 onto R4 of $K_V1.2$. This is in line with alignments proposed by previous studies [Ramsey et al., 2010, Gonzalez et al., 2010].

Two previous experimental studies proposed that the depolarization-driven outward motion of S4 replaces S4 arginines with N4 in the pore to open the channel [Tombola et al., 2008, Gonzalez et al., 2010], but another study found voltage-gating to be preserved without both R3 and N4 [Sakata et al., 2010], leaving the gating mechanism unresolved. Our findings would suggest that a truncated S4 lacking residue R3 would either lose proton selectivity or have to open in another position of S4, which placed a remaining arginine into the narrow part of the pore.

In conclusion, our results suggest that R3 enters a short narrow segment of the pore in the open state, where it interacts with D112, and that together these residues assemble to form the selectivity filter for the channel. We propose that the pore of hHv1 runs through its VSD, along the pathway taken by the S4 arginines, and that gating of the pore involves the formation of the selectivity filter in the activated conformation of S4.

EXPERIMENTAL PROCEDURES

DNA constructs and expression in Xenopus oocytes

Site directed mutagenesis was made by PCR using QuickChange mutagenesis (Stratagene, La Jolla, CA) and verified by subsequent sequencing. DNA was linearized with Nhe1 and transcribed using the T7 mMessage mMachine kit (Ambion, Austin, TX). *Xenopus laevis* oocytes were injected with 50 nl of RNA, concentrated at 0.25 – 2 μg/μl and incubated at 18 °C for 2 – 10 days in ND96, containing 96 mM NaCl, 2 mM KCl, 1.8 mM $CaCl_2$, 1 mM $MgCl_2$, 10 mM Hepes, 5 mM pyruvate, 100 mg/L gentamycin, pH 7.4.

Electrophysiological recordings

Prior to patch clamp recordings, oocytes were mechanically devitellinated under a stereoscope, and placed in a recording chamber under an inverted IX70 or IX71 microscope (Olympus, FI, Japan). Patch electrodes were pulled from G150TF-4 capillaries (Warner Instruments, Hamden, CT) on a P97 Micropipette Puller (Sutter, Novato, CA) and

extensively fire polished. Excised patches in the inside-out or outside-out configuration were obtained with an initial electrode resistance of 0.25 – 7 MΩ, depending on the pipette solution. Holding potentials were −60 or −80 mV. Recordings were performed at room temperature (22 – 25 °C) with an Axopatch 200B or 200A amplifier (Molecular Devices, Union City, CA), connected via a Digidata 1440A acquisition board to a PC running pClamp 10 (Molecular Devices). Data were filtered at 2 or 5 kHz and the sampling rate was 10 kHz. Pipette (extracellular) and bath (intracellular) solutions void of metallic cations at pH 6 were done with 100 mM 2-(N-morpholino)ethanesulfonic acid (MES), 30 mM Methanesulfonic acid (MS), 5 mM Tetraethylammonium Chloride (TEACl), 5 mM ethyleneglycol-bis(2-aminoethyl)-N,N,N’,N’-tetra-acetic acid (EGTA), adjusted to pH 6 with TEA hydroxide (> 25 mM). MES was replaced by 2-Amino-2-hydroxymethyl-propane-1,3-diol (TRIS) or 2-[4-(2-hydroxyethyl)piperazin-1-yl]ethanesulfonic acid (HEPES) for solutions adjusted pH 8 and 7, respectively. The guanidinium containing solution contained 100 mM GuHCl, 10 mM tris(hydroxymethyl)aminomethane (Tris), and 1 mM 2,2′,2″,2‴-(Ethane-1,2-diyldinitrilo)-tetra-acetic acid (EDTA), adjusted to pH 8 with HCl. GuHCl was replaced by NaCl, KCl, LiCl, or CsCl to test for the respective permeability ratios. Chemicals were bought from Sigma-Aldrich (St. Louis, MO) or Fischer Scientific (Waltham, MA). MTSET was bought from Toronto Research Chemicals (North York, ON).

Data analysis

Data were analyzed using Igor Pro (Wavemetrics, Portland, OR) or MATLAB (The Mathworks, Natick, MA). Tail currents for GV calculations were measured 5 – 100 ms after the end of the depolarizing voltage step, depending on the kinetics of the tail current. Leak subtraction was performed offline. GVs were fitted with a single Boltzmann with Igor Pro. Outward current amplitudes were measured just prior to the end of the depolarizing voltage step. To determine the reversal potential (Nernst potential) of tail currents at symmetric, asymmetric, or bi-ionic conditions (Figures 2, 8, S3), various holding potentials were applied after an activating voltage step (+100 mV), as shown in Figure 2C,D. Then, IVs were fitted with a cubic, and the zero crossing (Nernst potential) was determined analytically. Residues of the alignment in Figure 1B were colored with Jalview 2 [Waterhouse et al., 2009] in Zappo color scheme (hydrophobic I, L, V, A, and M = pink, aromatic F, W, and Y = orange, positively charged K, R, and H = red, negatively charged D and E = blue, hydrophilic S, T, N, and Q = green, P and G = magenta, C = yellow). Values are reported as mean ± s.e.m.

Supplementary Material

Refer to Web version on PubMed Central for supplementary material.

Acknowledgments

We would like to thank H. Okada and W. Chu for help with the cloning and the members of the Isacoff lab for discussion. This work was supported by postdoctoral fellowships for prospective and advanced researchers from the Swiss National Science Foundation (SNSF; PBELP3-127855 and PA00P3_134163) (T.K.B.) and by a grant from the National Institutes of Health (R01 NS35549) (E.Y.I.).

REFERENCES

Baker OS, Larsson HP, Mannuzzu LM, Isacoff EY. Three transmembrane conformations and sequence-dependent displacement of the s4 domain in shaker k+ channel gating. Neuron. 1998; 20(6):1283–1294. [PubMed: 9655514]

DeCaen PG, Yarov-Yarovoy V, Zhao Y, Scheuer T, Catterall WA. Disulfide locking a sodium channel voltage sensor reveals ion pair formation during activation. Proc Natl Acad Sci U S A. 2008; 105(39):15142–15147. [PubMed: 18809926]

DeCoursey TE. Voltage-gated proton channels and other proton transfer pathways. Physiol Rev. 2003; 83(2):475–579. [PubMed: 12663866]

DeCoursey TE. Voltage-gated proton channels. Cell Mol Life Sci. 2008; 65(16):2554–2573. [PubMed: 18463791]

DeCoursey TE, Morgan D, Cherny VV. The voltage dependence of nadph oxidase reveals why phagocytes need proton channels. Nature. 2003; 422(6931):531–534. [PubMed: 12673252]

Gamal El-Din TM, Heldstab H, Lehmann C, Greeff NG. Double gaps along shaker s4 demonstrate omega currents at three different closed states. Channels (Austin). 2010; 4(2)

Gonzalez C, Koch HP, Drum BM, Larsson HP. Strong cooperativity between subunits in voltage-gated proton channels. Nat Struct Mol Biol. 2010; 17(1):51–56. [PubMed: 20023639]

Henderson LM, Chappell JB, Jones OT. The superoxide-generating nadph oxidase of human neutrophils is electrogenic and associated with an h+ channel. Biochem J. 1987; 246(2):325–329. [PubMed: 2825632]

Koch HP, Kurokawa T, Okochi Y, Sasaki M, Okamura Y, Larsson HP. Multimeric nature of voltage-gated proton channels. Proc Natl Acad Sci U S A. 2008; 105(26):9111–9116. [PubMed: 18583477]

Larsson HP, Baker OS, Dhillon DS, Isacoff EY. Transmembrane movement of the shaker k+ channel s4. Neuron. 1996; 16(2):387–397. [PubMed: 8789953]

Lee S-Y, Letts JA, MacKinnon R. Dimeric subunit stoichiometry of the human voltage-dependent proton channel hv1. Proc Natl Acad Sci U S A. 2008; 105(22):7692–7695. [PubMed: 18509058]

Lee S-Y, Letts JA, MacKinnon R. Functional reconstitution of purified human hv1 h+ channels. J Mol Biol. 2009; 387(5):1055–1060. [PubMed: 19233200]

Li SJ, Zhao Q, Zhou Q, Unno H, Zhai Y, Sun F. The role and structure of the carboxyl-terminal domain of the human voltage-gated proton channel hv1. J Biol Chem. 2010; 285(16):12047–12054. [PubMed: 20147290]

Long SB, Tao X, Campbell EB, MacKinnon R. Atomic structure of a voltage-dependent k+ channel in a lipid membrane-like environment. Nature. 2007; 450(7168):376–382. [PubMed: 18004376]

Musset B, Smith SME, Rajan S, Morgan D, Cherny VV, DeCoursey TE. Aspartate112 is the selectivity filter of the human voltage-gated proton channel. Nature. 2011 doi: 10.1038/nature10557. [Epub ahead of print].

Ramsey IS, Mokrab Y, Carvacho I, Sands ZA, Sansom MSP, Clapham DE. An aqueous h+ permeation pathway in the voltage-gated proton channel hv1. Nat Struct Mol Biol. 2010; 17(7):869–875. [PubMed: 20543828]

Ramsey IS, Moran MM, Chong JA, Clapham DE. A voltage-gated proton-selective channel lacking the pore domain. Nature. 2006; 440(7088):1213–1216. [PubMed: 16554753]

Ramsey IS, Ruchti E, Kaczmarek JS, Clapham DE. Hv1 proton channels are required for high-level nadph oxidase-dependent superoxide production during the phagocyte respiratory burst. Proc Natl Acad Sci U S A. 2009; 106(18):7642–7647. [PubMed: 19372380]

Sakata S, Kurokawa T, Nørholm MHH, Takagi M, Okochi Y, von Heijne G, Okamura Y. Functionality of the voltage-gated proton channel truncated in s4. Proc Natl Acad Sci U S A. 2010; 107(5):2313–2318. [PubMed: 20018719]

Sasaki M, Takagi M, Okamura Y. A voltage sensor-domain protein is a voltage-gated proton channel. Science. 2006; 312(5773):589–592. [PubMed: 16556803]

Sokolov S, Scheuer T, Catterall WA. Ion permeation through a voltage-sensitive gating pore in brain sodium channels having voltage sensor mutations. Neuron. 2005; 47(2):183–189. [PubMed: 16039561]

Sokolov S, Scheuer T, Catterall WA. Gating pore current in an inherited ion channelopathy. Nature. 2007; 446(7131):76–78. [PubMed: 17330043]

Sokolov S, Scheuer T, Catterall WA. Depolarization-activated gating pore current conducted by mutant sodium channels in potassium-sensitive normokalemic periodic paralysis. Proc Natl Acad Sci U S A. 2008; 105(50):19980–19985. [PubMed: 19052238]

Sokolov S, Scheuer T, Catterall WA. Ion permeation and block of the gating pore in the voltage sensor of nav1.4 channels with hypokalemic periodic paralysis mutations. J Gen Physiol. 2010; 136(2): 225–236. [PubMed: 20660662]

Starace DM, Bezanilla F. Histidine scanning mutagenesis of basic residues of the s4 segment of the shaker k+ channel. J Gen Physiol. 2001; 117(5):469–490. [PubMed: 11331357]

Starace DM, Bezanilla F. A proton pore in a potassium channel voltage sensor reveals a focused electric field. Nature. 2004; 427(6974):548–553. [PubMed: 14765197]

Struyk AF, Markin VS, Francis D, Cannon SC. Gating pore currents in diis4 mutations of nav1.4 associated with periodic paralysis: saturation of ion flux and implications for disease pathogenesis. J Gen Physiol. 2008; 132(4):447–464. [PubMed: 18824591]

Tiwari-Woodruff SK, Lin MA, Schulteis CT, Papazian DM. Voltage-dependent structural interactions in the shaker k(+) channel. J Gen Physiol. 2000; 115(2):123–138. [PubMed: 10653892]

Tombola F, Pathak MM, Gorostiza P, Isacoff EY. The twisted ion-permeation pathway of a resting voltage-sensing domain. Nature. 2007; 445(7127):546–549. [PubMed: 17187057]

Tombola F, Pathak MM, Isacoff EY. Voltage-sensing arginines in a potassium channel permeate and occlude cation-selective pores. Neuron. 2005; 45(3):379–388. [PubMed: 15694325]

Tombola F, Pathak MM, Isacoff EY. How does voltage open an ion channel? Annu Rev Cell Dev Biol. 2006; 22:23–52. [PubMed: 16704338]

Tombola F, Ulbrich MH, Isacoff EY. The voltage-gated proton channel hv1 has two pores, each controlled by one voltage sensor. Neuron. 2008; 58(4):546–556. [PubMed: 18498736]

Tombola F, Ulbrich MH, Kohout SC, Isacoff EY. The opening of the two pores of the hv1 voltage-gated proton channel is tuned by cooperativity. Nat Struct Mol Biol. 2010; 17(1):44–50. [PubMed: 20023640]

Waterhouse AM, Procter JB, Martin DMA, Clamp M, Barton GJ. Jalview version 2–a multiple sequence alignment editor and analysis workbench. Bioinformatics. 2009; 25(9):1189–1191. [PubMed: 19151095]

Wood ML, Schow EV, Freites JA, White SH, Tombola F, Tobias DJ. Water wires in atomistic models of the hv1 proton channel. Biochim Biophys Acta. 2011

Yang N, George AL, Horn R. Molecular basis of charge movement in voltage-gated sodium channels. Neuron. 1996; 16(1):113–122. [PubMed: 8562074]

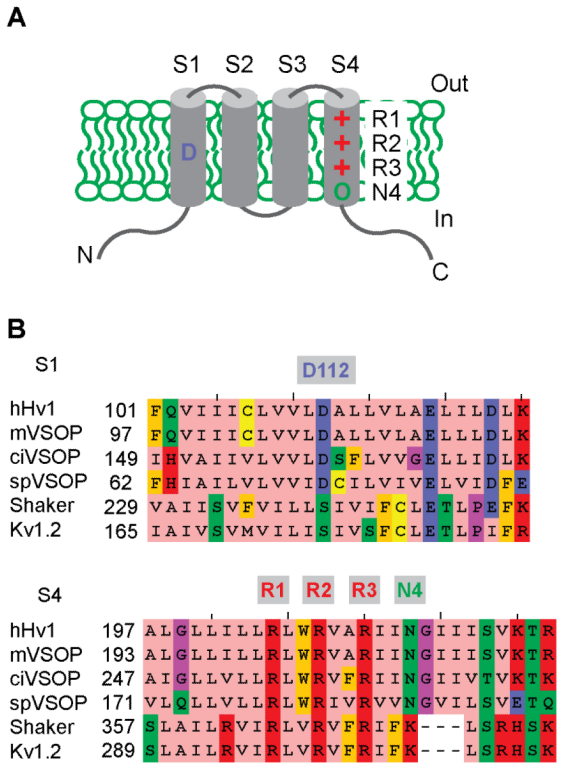

Figure 1. Cartoon and sequence alignment of the human voltage gated proton channel (hHv1)

A, Membrane topology model of hHv1, with specific residues emphasized: D112 in S1, R205 (R1), R208 (R2), R211 (R3) and N214 (N4) in S4. **B**, sequence alignment of voltage-gated proton channels (human hHv1, mouse mVSOP, *Ciona intestinales* ciVSOP, and *Strongylocentrotus purpuratus* spVSOP) and voltage gated K^+ channels (Shaker and Kv1.2).

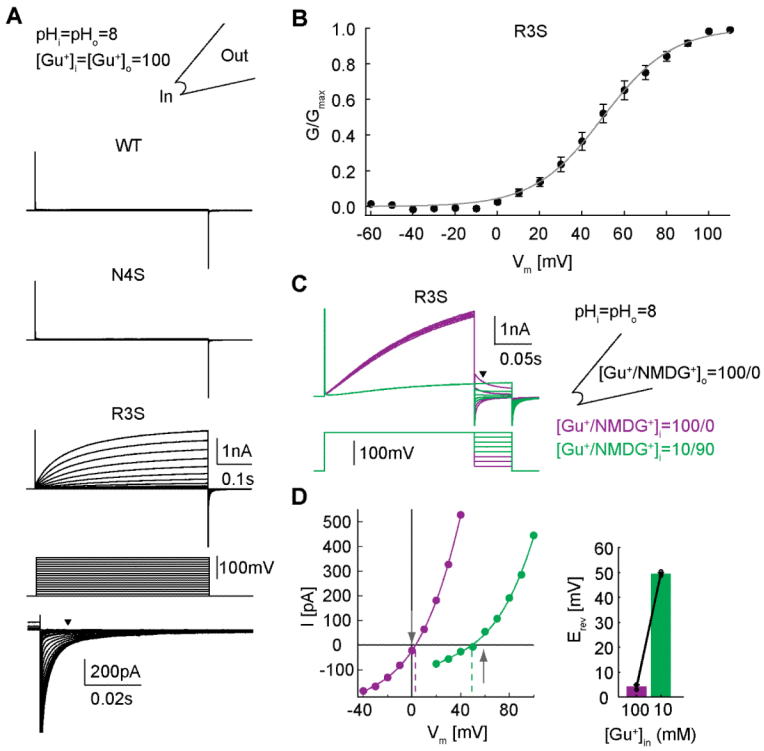

Figure 2. The R3S mutant conducts guanidinium ions

A, *Top*, inside-out patches of R3S have large outward currents upon depolarization and inward tail currents upon repolarization in 100 mM symmetric $[Gu^+]_i = [Gu^+]_o$, whereas WT and N4S have no detectable currents. *Bottom*, tail currents of R3S. **B**, conductance-voltage relationship (n = 8), fitted Boltzmann ($V_{1/2}$ = 50.17 ± 3.31 mV and kT/ze_0 = 15.25 ± 0.68 mV). Error bars denote s.e.m. **C**, Tail currents at various holding potentials for symmetric $[Gu^+]_i = [Gu^+]_o$ = 100 mM (purple traces) and asymmetric $[Gu^+]_i$ = 10 mM, $[NMDG^+]_i$ = 90 mM, $[Gu^+]_o$ = 100mM conditions (green traces). Triangles mark current measurement time point for current-voltage relation. **D**, *Left*, example of a current-voltage relation of tail currents. Arrows mark expected reversal potentials for pure Gu^+ selectivity (0 mV for symmetric and 58.76 mV for asymmetric condition, dashed lines mark actual zero crossings. *Right*, interpolated reversal potentials for symmetric and asymmetric conditions are significantly different ($E_{rev\ sym}$ = 4.20 ± 1.10 mV, $E_{rev\ asym}$ = 49.50 ± 0.83 mV, n = 3, paired t-test, $p < 0.01$; error bars denote s.e.m). Bar graphs display the mean. Data points are shown as circles connected by lines for each individual patch. Similarity between predicted and observed reversal potentials indicates that Gu^+ is the major charge carrying ion through R3S at pH 8.

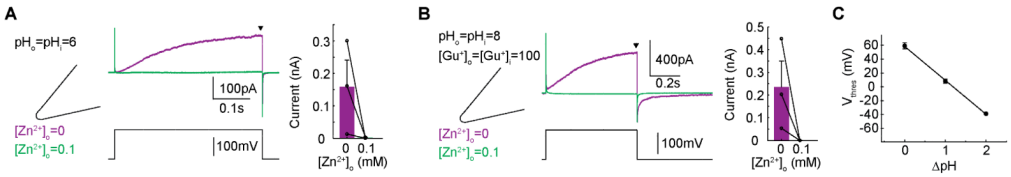

Figure 3. The R3S mutant retains hallmark properties of WT hHv1

A, Proton conduction by R3S mutant is efficiently blocked by external application of 100 μM Zn^{2+}. A voltage step from −80 mV to 100 mV was applied to outside-out patches with (green traces and bars) or without (purple traces and bars) external 100 μM Zn^{2+}. Bar graphs display the mean outward current (measured at the end of the depolarizing voltage step, as indicated by an arrow). Data points are shown as circles connected by lines for each individual patch. **B**, Gu^+ conduction by R3S is blocked efficiently by external application of 100 μM Zn^{2+}. Same color code as in panel **A**. Error bars denote s.e.m. **C**, Mutant R3S preserves the ability to sense ΔpH gradient over the membrane. The slope is −48.9 ± 1.23 mV/pH unit.

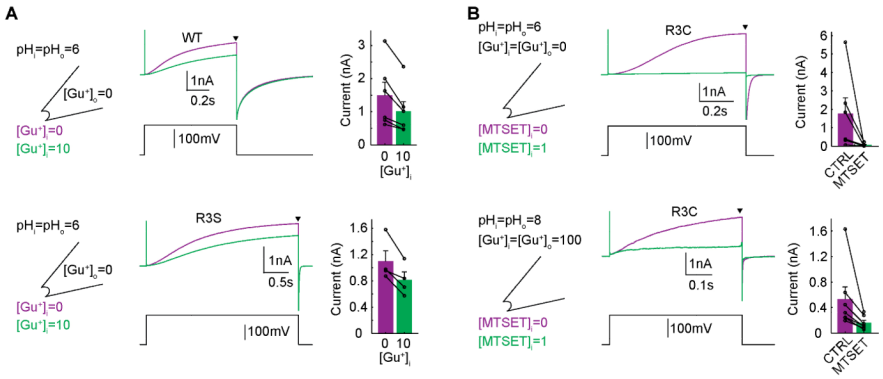

Figure 4. Protons take same pathway as guanidinium ions through R3S and R3C

A, Internal Gu^+ reduces outward proton current in symmetrical pH = 6 for both WT (top) and R3S (bottom), suggesting that Gu^+ enters and blocks the proton permeation pathway. A voltage step from −80 mV to 100 mV was applied to inside-out patches with (green traces and bars) or without (purple traces and bars) internal 10 mM Gu^+. **B**, Internal MTSET (1 mM) strongly reduces both proton conduction through R3C channels at pH 6 (top) and Gu^+ conduction at pH 8 (bottom). A voltage step from −80 mV to 100 mV applied before (purple traces and bars) and after (green traces and bars) bath application of 1 mM MTSET. In A and B, bar graphs display the mean outward current (measured at the end of the depolarizing voltage step, as indicated by an arrow).Data points are shown as circles connected by lines for each individual patch. Error bars denote s.e.m.

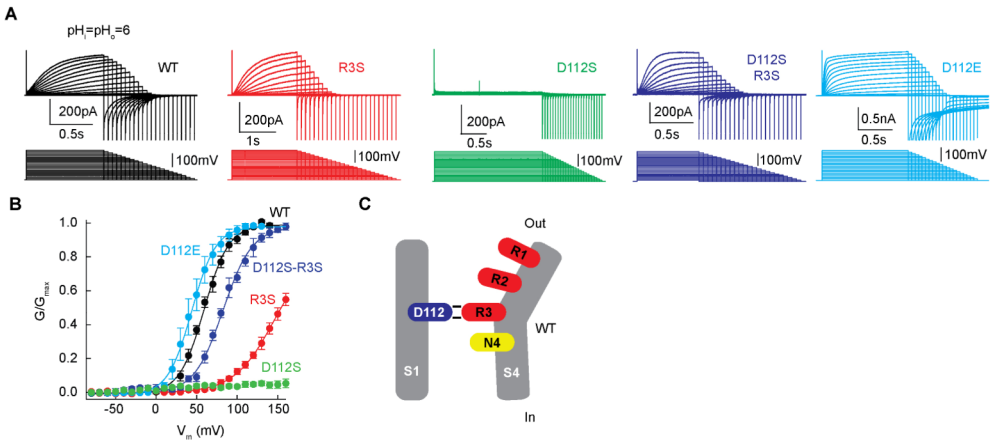

Figure 5. D112 interacts with R3

A, Proton currents in response to depolarizing step voltages in WT (black), R3S (red), D112S (green, n = 3), double mutant D112S-R3S (dark blue), and D112E (blue) at pH_i = pH_o = 6. Holding potential was −80 mV. **B,** G-V relationships of WT and mutant channels. D112S is normalized to WT G_{max}. Single Boltzmann fits, WT: $V_{1/2}$ = 59.28 ± 2.34 mV, kT/ze_0 = 15.27± 0.61 mV, n = 3; R3S: $V_{1/2}$ = 146.47 ± 4.1 mV, kT/ze_0 = 24.92 ± 0.8 mV, n = 6; D112S-R3S: $V_{1/2}$ = 82.65± 3.26 mV, kT/ze_0 = 17.86 ± 1.2 mV, n = 5; D112E: $V_{1/2}$ = 44.03 ± 6 mV, kT/ze_0 = 14.86 ± 0.77 mV, n = 4. Error bars denote s.e.m. **C**, Model of hHv1 shows S4 stabilized in activated state when the positively charged R3 approaches the negatively charged D112 (WT).

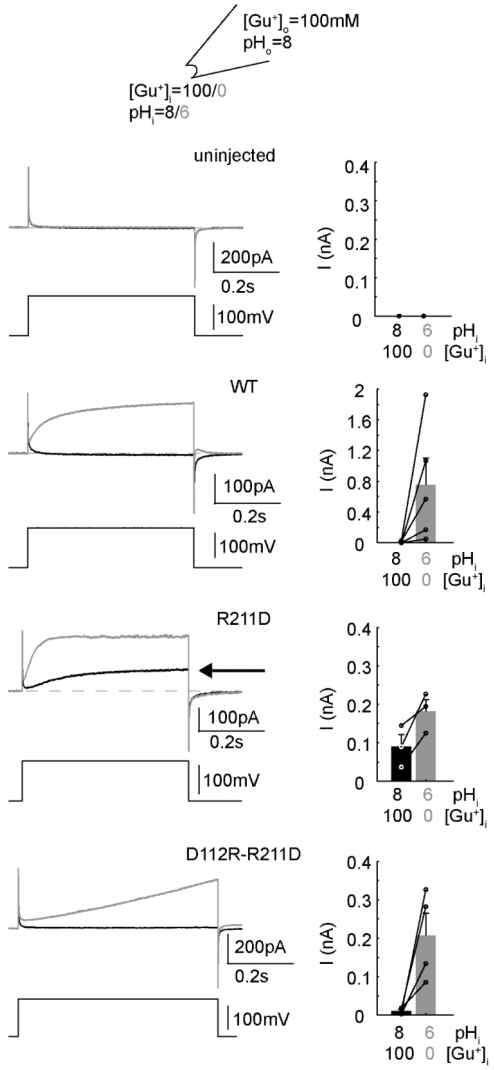

Figure 6. Like WT, the charge-swapped double mutant D112R-R3D does not conduct Gu^+

Inside-out patches were initial recorded in symmetric 100 mM Gu^+ pH 8 solution (black traces), and subsequently internally perfused with 0 mM Gu^+ pH 6 solution. Mutant R3D displays an outward current in symmetric Gu solution (marked by an arrow), whereas WT and D112R-R3D do not. Relative maximal outward current reduction by 100 mM Gu pH 8 vs 0 mM Gu pH6 was 99.1 ± 0.7 % for WT, 52.2 ± 13.6 % for D112R-R3D, and 92.3 ± 4.7 % for D112R-R3D. Bar graphs display the mean outward current (measured at the end of the depolarizing voltage step). Data points are shown as circles connected by lines for each individual patch. Errors bars denote s.e.m.

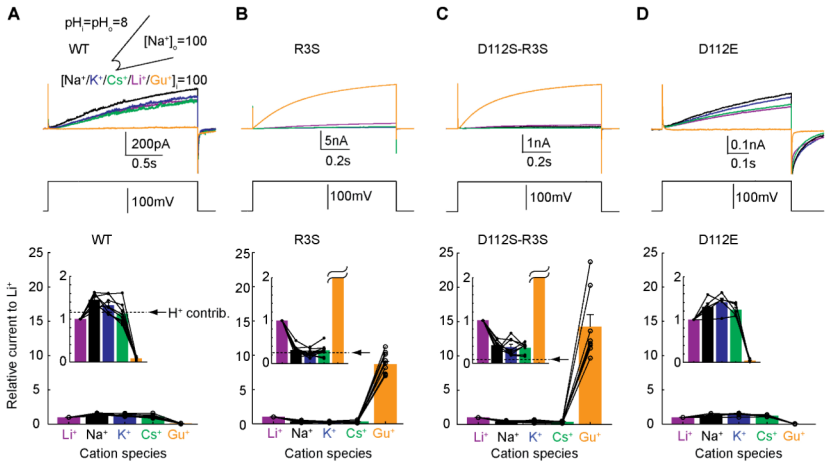

Figure 7. R3 and D112 influence metal cation conduction

A-D, Normalized representative traces (*upper*) and average amplitudes normalized to Li^+ (*lower*) of outward currents, in presence and absence of metal cations or Gu^+ during depolarization to +60 mV in inside-out patches of WT (**A**), R3S (**B**), D112S-R3S (**C**) and D112E (**D**). Bar graphs display the mean outward current (measured at the end of the depolarizing voltage step). Data points are shown as circles connected by lines for each individual patch. Recordings began in $[Na^+]_i = [Na^+]_o = 100$ mM at pH 8 (black traces) and bath (internal) solution was then changed to 100 mM K^+, Li^+, Cs^+, and Gu^+ at pH 8 (blue, purple, green, and orange). Fraction of current carried by protons (see Figure S5) shown in the insets (zoom in) as dashed lines. Note that R3S and D112S-R3S differ in profile from WT and from each other, indicating that both R3 and D112 contribute to selectivity. Error bars denote s.e.m.

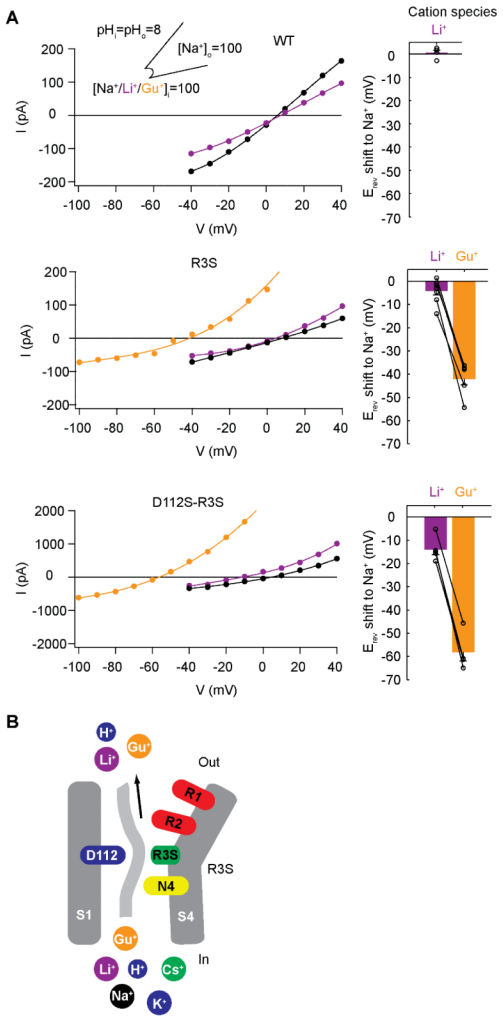

Figure 8. R3 and D112 line the pore and determine cation selectivity

A, Reversal potentials E_{rev} measured by a serious of holding potentials after an activating depolarizing step voltage (+100 mV for 0.2 s, same protocol as depicted in Figure 2C) for inside-out patches of WT, R3S, and D112S-R3S. Recordings began in $[Na^+]_i$ = $[Na^+]_o$ = 100 mM at pH 8 and bath (internal) solution was then changed to 100 mM Li^+ and/or Gu^+ at pH 8. Bar graphs depict the shift of mean E_{rev} after cation change. Data points are shown as circles connected by lines for each individual patch. **B**, Model of the selectivity filter of hHv1 consisting of R3 and D112 as inferred from our data. Error bars denote s.e.m.